Electronic Supplementary information

Characterization of drug–drug salt forms of metformin and aspirin with improved physicochemical properties

Wen-Xiu Zhou,[ab] Hong-Wei Zhao,[ab] Huan-Huan Chen,[ab] Zai-Yong Zhang[a] and Dong-Ying Chen*[a]

[a] *Research Center for Pharmaceutical Quality Control and Solid-State Chemistry, Shanghai Institute of Materia Medica, Chinese Academy of Sciences, 555 Rd. Zuchongzhi, Zhangjiang Hi-Tech Park, Shanghai, 201203, China. E-mail: dychen@simm.ac.cn*

[b] *University of Chinese Academy of Sciences, Beijing 100049, China.*

Experimental Section

S1.1. Materials

Aspirin (ASP) was purchased from Sinopharm Chemical Reagent Company (Shanghai, China) and used as received. Metformin (MET) was prepared by adding metformin hydrochloride (1.65 g, 10 mmol) and sodium hydroxide (0.4 g, 10 mmol) into 100 mL ethanol and the suspension was filtered after stirring at ambient temperature for 24 hours followed by removing solvent with the rotary evaporator. Water with a resistivity of 18.2 MΩ. cm was prepared by a Milli-Q plus system Millipore AS. HPLC grade acetonitrile was obtained from Sigma-Aldrich (St. Louis, MO, USA). All other reagents were of analytical grade (Sinopharm Chemical Reagent Co., Ltd, Shanghai, China), and used without any further purification.

S1.2. Preparation of MET-ASP Anhydrate

1.3 g freshly prepared MET and 1.8 g ASP were dissolved in 50 mL acetone, the anhydrate powders precipitated with continuous stir. The filtrate was kept in a refrigerator at 4 °C for 24 hours, which yielded single crystals of anhydrate that were suitable for SCXRD analysis.

S1.3. Preparation of MET-ASP Hemihydrate

Hemihydrate was prepared by exposing the powder samples of anhydrate to 95% RH condition which was achieved within a sealed desiccator containing the saturated potassium nitrate for 4 hours. A single crystal suitable for SCXRD studies was also obtained simultaneously at the edges of the powders.

S1.4. Power X-ray Diffraction (PXRD)

PXRD patterns were obtained using a Bruker D8 Advance X-ray diffractometer coupled with a Cu-Kα radiation (λ = 1.5418 Å). Voltage and current of the generator were set at 40 kV and 40 mA, respectively. Data over the 2θ range of 3−40° were collected with a scan speed of 15°/min (step size 0.025°, step time 0.1 s) at ambient temperature. Data were imaged and integrated with RINT Rapid and peak-analyzed with Jade 6.0 software from Rigaku.

S1.5. Thermal Analysis

Thermogravimetric analysis (TGA) was carried out on a Netzsch TG 209F3 equipment under nitrogen gas (20 mL/min) at a scan rate of 10 °C/min from 30 to 400 °C. Differential scanning calorimetry (DSC) was performed with a DSC TA Q2000 instrument, the sample was placed in non-hermetic aluminium pan that was crimped with an aligned cover and heated under a heating rate 10 °C/min with nitrogen gas flow of 50 mL/min. For TGA and DSC, typical samples of weighing 2-5 mg were used.

S1.6. Single-Crystal X-ray Data Collection and Structure Determinations

Single crystal X-ray diffraction measurements were performed on a Bruker Smart Apex II diffractometer, using Mo-Kα radiation ($\lambda = 0.71073$ Å) with a graphite monochromator at 205 K. The integration and scaling of the intensity data were accomplished using the SAINT program. The data were corrected for effects of absorption using SADABS. The structures were solved by direct methods and refined with full-matrix least-squares technique using the SHELX-2014 software. Hydrogen atoms of N–H and O–H were located from different electron density maps, and hydrogen atoms of C–H were placed in calculated positions and refined with a riding model. Non-hydrogen atoms were refined with anisotropic displacement parameters The data with .cif format have been deposited in the Cambridge Crystallographic Data Center, CCDC NO. 1860886 and 1860888 for the anhydrate and hemihydrate of MET-ASP, respectively.

S1.7. Fourier-Transform Infrared Spectroscopy (FTIR)

Fourier transform infrared (FTIR) spectra were collected by a Nicolet 6700 FT-IR spectrometer in the range from 4000 to 400 cm^{-1} with a resolution of 4 cm^{-1} under ambient conditions. The IR spectra were recorded on samples dispersed in KBr pellets.

S1.8. Dynamic Vapor Sorption (DVS)

The water sorption and desorption processes were measured on an Intrinsic DVS instrument. Samples were mounted on a balance and studied over a humidity range from 0 to 80% RH at 25 °C. Each humidity step was made if less than a 0.02% weight change occurred in 10 minutes, with a maximum hold time of 3 hours.

S1.9. Scanning Electron Microscopy (SEM)

The surface morphology of the single crystals of anhydrate stored under 95% RH were periodically viewed using scanning electron microscopy (Agilent 8500) operated at a beam voltage of 1kV. The samples were mounted onto a steel stage using double-sided adhesive tape before the analysis.

S1.10. Polarized Light Microscopy

Single crystal of anhydrate was fixed on a glass slide, stored at 95% RH, and periodically observed with Olympus SZ61 microscope with dual polarizer. The image was processed using S-EYE software.

S1.11. Face Indexing of Anhydrate Single Crystal

A single crystal of anhydrate was mounted on a glass capillary in a Bruker Smart Apex II diffractometer for data collection using Mo-Kα radiation ($\lambda = 0.71073$ Å) with a graphite monochromator at 205 K. The face indexing was performed using the APEX-3 program.

S1.12. Intrinsic Dissolution Rate Analysis

Intrinsic dissolution rate (IDR) experiments were carried out on a Mini IDR apparatus. A quantity of 5-30 mg of each sample was compressed at an average compression force of 30 bar for 30 seconds to make non-disintegrating compacts using die and punch with the surface area of 0.07 cm^2. Dissolution study was conducted using 10 mL 0.1N HCl solution as the dissolution medium at 37 °C with rotating disk speed at 100 rpm. 200 µL of the samples were withdrawn at 5, 10, 15, 20, 25, 30 minutes. The concentration was determined by high-performance liquid chromatography (HPLC) which was conducted on Shimadzu LC-20 equipped with a UV detector with the wavelength set at 233 nm. A Discovery C18 column (150x4.6 mm i.d., 5 µm particle size) was employed with the mobile phase consisting of 20 mM sodium 1-heptanesulfonate (the pH value was adjusted to 2.8 with glacial acetic acid) and acetonitrile with the ratio of 80:20 (v/v) under the flow rate of 1.0 mL·min^{-1}.

S2. Results

Table S1 Crystallographic data and refinement details for MET-ASP.

	Anhydrate	Hemihydrate
Chemical formula	$C_9H_7O_4 \cdot C_4H_{12}N_5$	$C_9H_7O_4 \cdot C_4H_{12}N_5 \cdot 1/2H_2O$
M_r	309.33	318.34
Crystal system	Monoclinic	Triclinic
Space group	$P2_1/c$	P-1
Temperature (K)	205	205
a (Å)	9.982 (4)	9.0858 (9)
b (Å)	10.918 (3)	11.9718 (12)
c (Å)	15.273 (2)	16.5784 (17)
α (°)	90.000	69.900 (1)
β (°)	107.315 (5)	75.107 (2)
γ (°)	90.000	67.877 (3)
V (Å^3)	1589.1 (8)	1551.8 (3)
D_{Cal} (g/cm^3)	1.293	1.363
Z	4	2
Radiation type	Mo $K\alpha$	Mo $K\alpha$

R_{int}	0.063	0.048
$R[F^2 > 2\sigma(F^2)]$	0.050	0.054
$wR(F^2)$	0.151	0.137
S	1.07	0.96
No. of reflections	3610	6965
$\Delta\rho_{max}$ (e Å^{-3})	0.23	0.22
$\Delta\rho_{min}$ (e Å^{-3})	-0.26	-0.25
CCDC no.	1860886	1860888

Table S2 Hydrogen bonds for the anhydrate of MET-ASP.

D–H···A(Å)	D–H(Å)	H···A (Å)	D···A (Å)	D–H···A(deg)	Symmetry code
N1–H1A···O4	0.87	1.98	2.842(3)	168	1-x, 1-y, 1-z
N1–H1B···O4	0.87	2.06	2.833(2)	148	-1+x, y, z
N2–H2A···O3	0.87	2.08	2.915(2)	161	1-x, 1-y, 1-z
N2–H2B···O3	0.87	2.17	2.836(2)	134	x, y, z
N2–H2B···N4[a]	0.87	2.50	2.907(3)	109	x, y, z
N4–H4A···N2[a]	0.87	2.49	2.907(3)	110	x, y, z
N4–H4B···O1	0.87	2.26	3.059(3)	153	3/2-x, -1/2+y, 3/2-z
C3–H3···O3	0.94	2.55	3.417(3)	153	1/2+x, 3/2-y, 1/2+z
C5–H5···O4[a]	0.94	2.44	2.762(3)	100	x, y, z
C12–H12C···N3[a]	0.97	2.29	2.738(3)	107	x, y, z

[a] Intramolecular hydrogen bond

Table S3 Hydrogen bonds for the hemihydrate of MET-ASP.

D–H···A (Å)	D–H (Å)	H···A (Å)	D···A (Å)	D–H···A (deg)	Symmetry code
N1′–H1′A···O3′	0.87	1.90	2.760(3)	169	1+x, y, z
N1–H1A···O4	0.83(3)	2.49(3)	3.198(3)	144(3)	-1+x, y, z
N1–H1B···O5	0.93(2)	2.10(2)	3.016(3)	168(2)	x, y, z
N1′–H1′B···N4′[a]	0.87	2.54	2.936(3)	109	x, y, z
N1′–H1′B···O3′	0.87	2.07	2.855(3)	150	1-x, 1-y, 2-z
N2–H2A···O4	0.87	2.00	2.843(3)	163	-1+x, y, z
N2–H2B···N3′	0.87	2.15	3.014(3)	175	-1+x, y, z
N2′–H2′A···O4′	0.87	2.31	3.175(3)	173	1+x, y, z
N2′–H2′B···N3	0.87	2.18	3.048(3)	176	1+x, y, z
N4–H4A···O3	0.95(3)	1.92(3)	2.841(3)	165(3)	x, y, z
N4–H4B···O4	0.93(2)	2.05(2)	2.919(3)	154(2)	1-x, 2-y, 1-z
O5–H5A···O1′	0.86	2.27	3.127(3)	172	1-x, 1-y, 1-z
O5–H5B···O3	0.86	1.95	2.777(3)	160	x, y, z
N4′–H4′A···O4′	0.91(2)	1.96(2)	2.862(3)	168(2)	x, y, z
N4′–H4′B···N1′[a]	0.89(2)	2.49(2)	2.936(3)	111.1(18)	x, y, z
C8′–H8′B···O2	0.97	2.52	3.465(4)	165	1-x, 1-y, 1-z
C12–H12A···O1	0.97	2.59	3.421(3)	144	x, y, z
C12–H12C···N4[a]	0.97	2.34	2.766(3)	105	x, y, z
C12′–H12D···N3′[a]	0.97	2.34	2.766(3)	106	x, y, z
C13–H13C···N3[a]	0.97	2.41	2.753(3)	100	x, y, z

[a] Intramolecular hydrogen bond

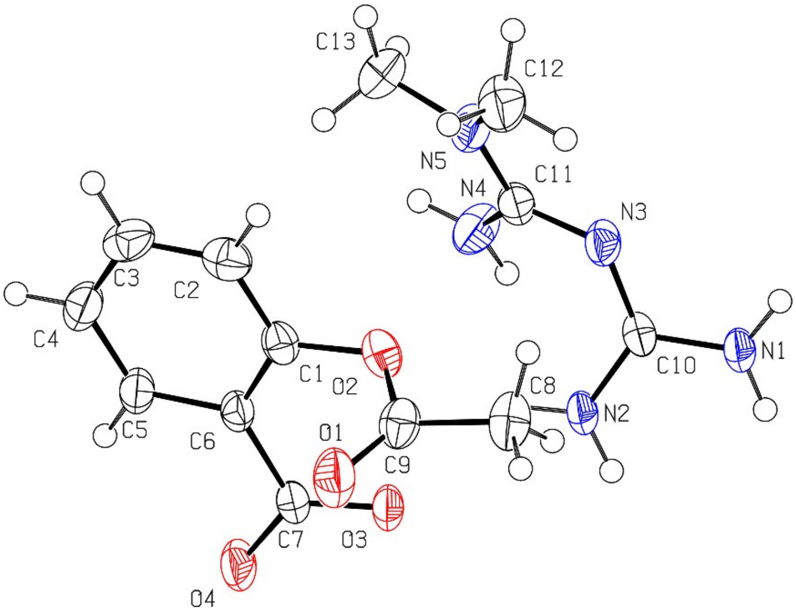

Figure S1 Thermal ellipsoid figure for the MET and ASP molecules of the anhydrate of MET-ASP drawn at 50% probability level.

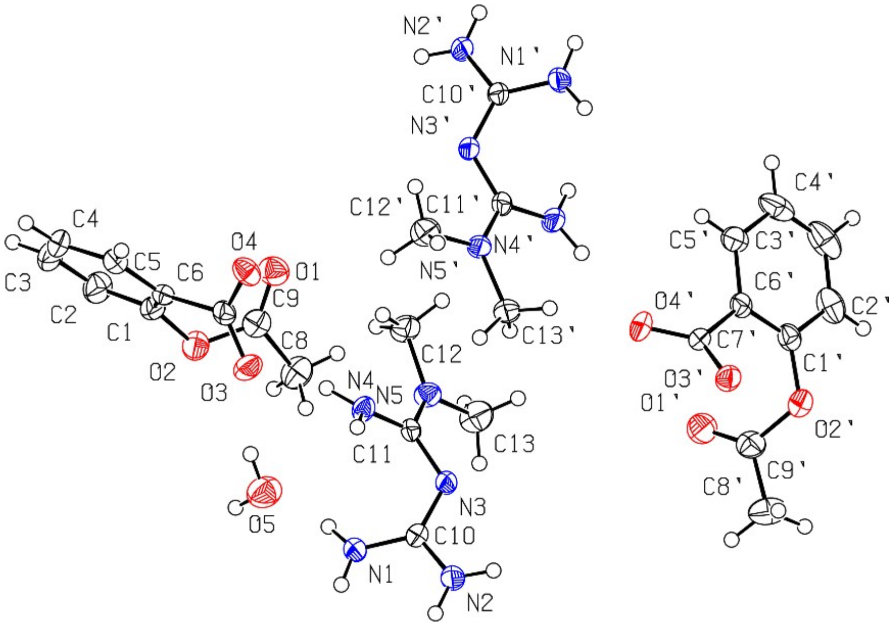

Figure S2 Thermal ellipsoid figure for the MET, ASP and water molecules of the hemihydrate of MET-ASP drawn at 50% probability level.

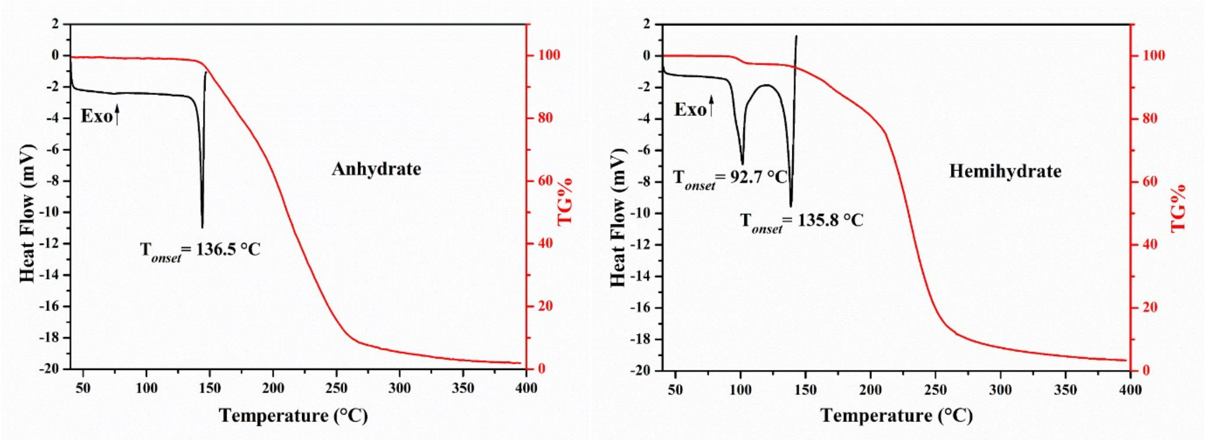

Figure S3 Thermal patterns of anhydrate and hemihydrate of MET-ASP. The red and black lines represent TGA and DSC curves, respectively.

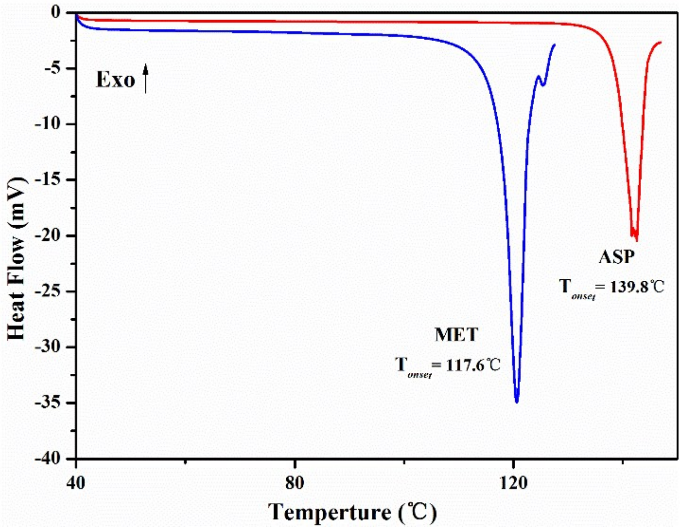

Figure S4 DSC thermograms of MET and ASP.

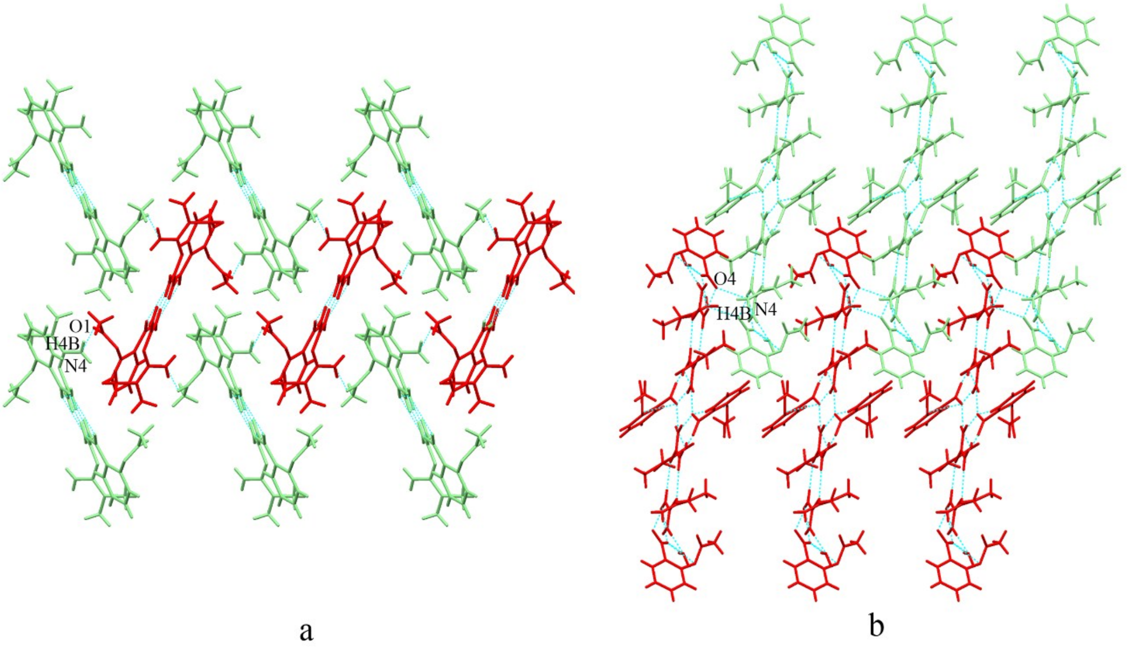

Figure S5 3D structure of MET-ASP, (a) anhydrate, (b) hemihydrate (view down the *a* axis).

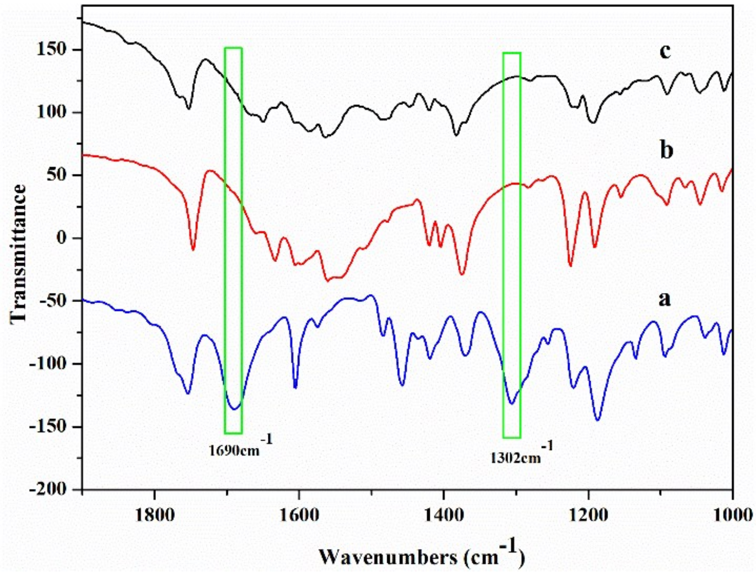

Figure S6 FTIR patterns for (a) ASP, (b) anhydrate and (c) hemihydrate of MET-ASP

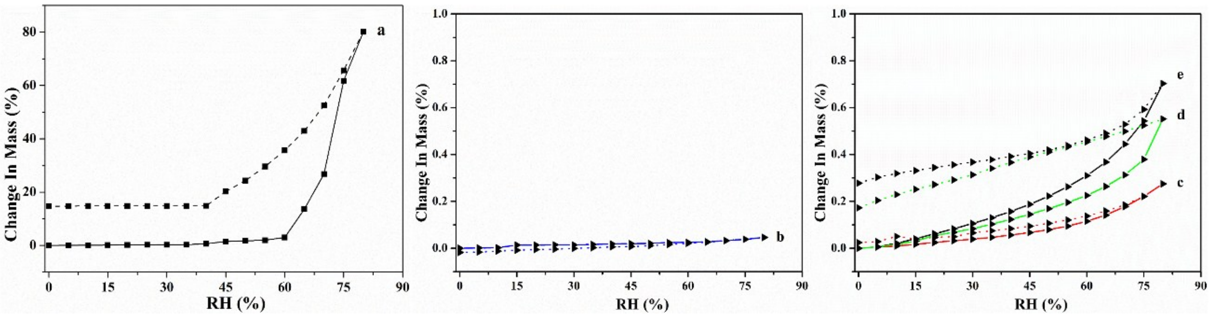

Figure S7 DVS charts of individual components (a) MET base, (b) ASP, (c) MET-HCl, (d) anhydrate and (e) hemihydrate of MET-ASP. The solid and dash lines represent water absorption and desorption, respectively.

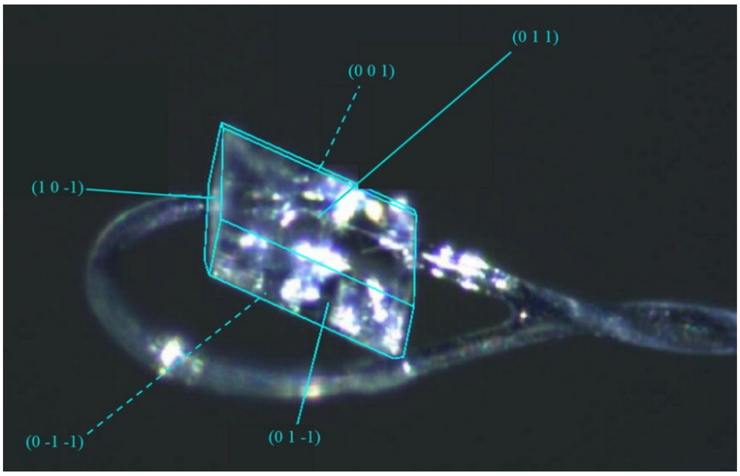

Figure S8 Face indexing of single crystal of MET-ASP anhydrate.

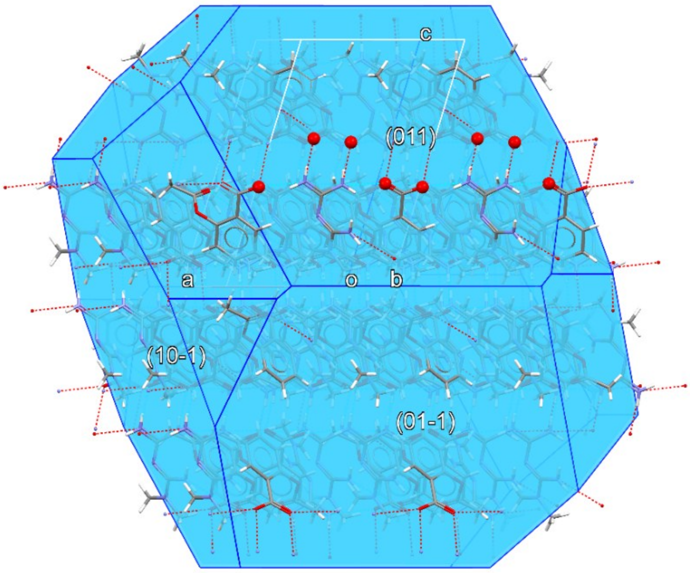

Figure S9 Crystal morphology of MET-ASP anhydrate deduced from the BFDH law.

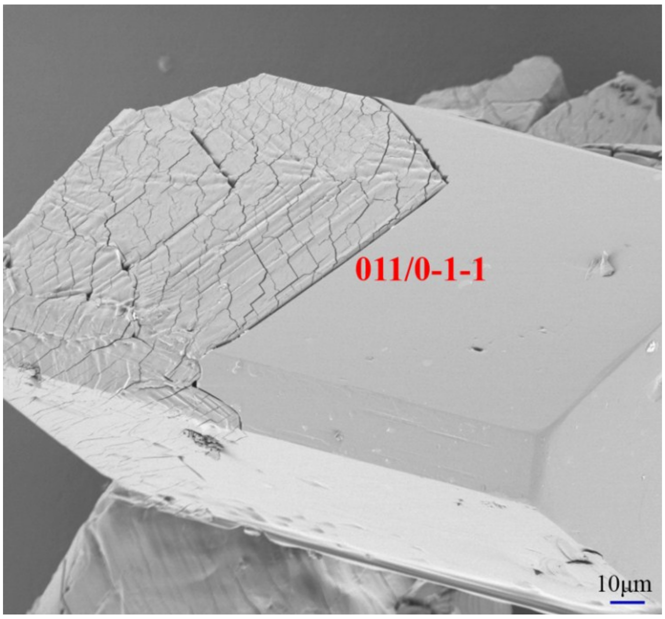

Figure S10 SEM image of single crystal of MET-ASP anhydrate under 95% RH for 2 hr.

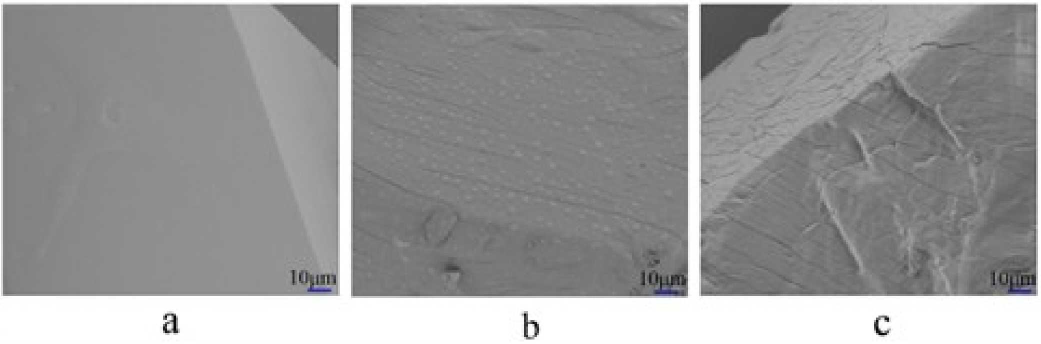

Figure S11 SEM images of anhydrate single crystals under 95% RH for (a) 0 hr, (b) 1 hr, and (c) 4 hr.

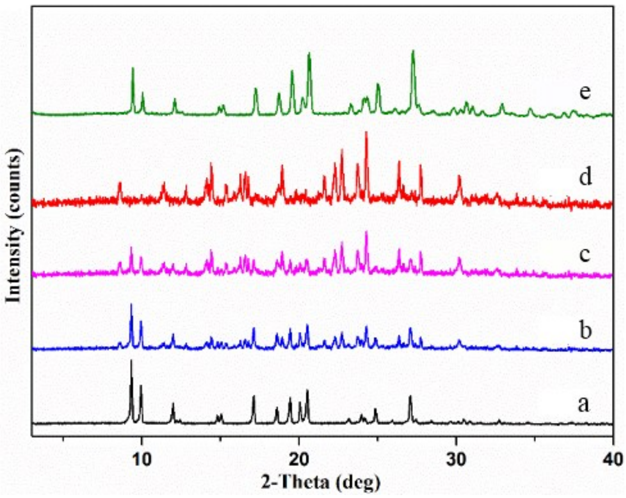

Figure S12 The PXRD patterns of anhydrate under 95% RH for (a) 0 hr, (b) 1 hr, (c) 2 hr, (d) 4 hr, and (e) hemihydrate heated under 90 °C for 2 min.

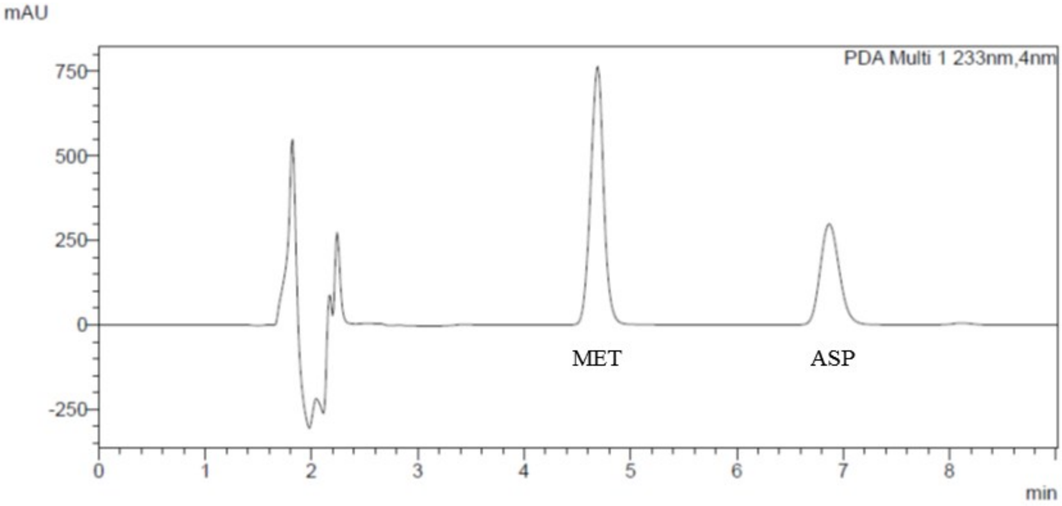

Figure S13 HPLC chromatogram of MET-ASP for IDR values determination.

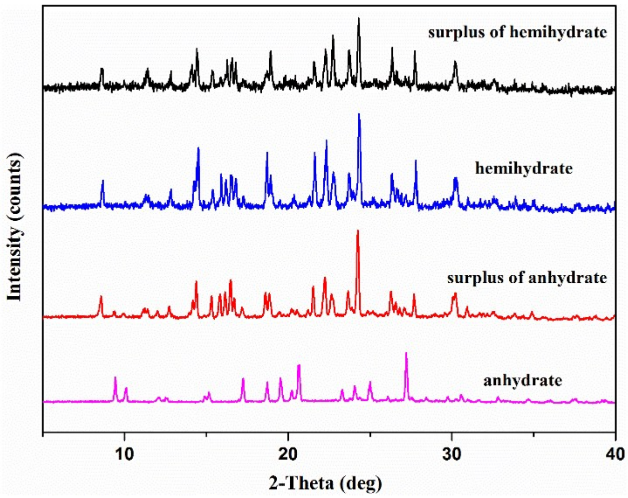

Figure S14 PXRD patterns of the surplus solids of MET-ASP after IDR experiments compared with those of original crystal forms.